Dynamic Accounting of Carbon Uptake in the Built Environment

Elisabeth Van Roijen, Seth Kane, Jin Fan, Josefine A Olsson, Baishakhi Bose, Thomas P Hendrickson, Sarah L Nordahl, Alissa Kendall, Corinne D Scown, Sabbie A Miller

Environmental Science & Technology

Received January 3, 2025
Accepted March 19, 2025
Published March 25, 2025

Please cite this article as:

Van Roijen, E., S, Kane, J. Fan, J.A. Olsson, B. Bose, T.P. Hendrickson, S.L. Nordahl, A. Kendall, C.D. Scown, S.A. Miller (2025). "Dynamic Accounting of Carbon Uptake in the Built Environment." *Environmental Science & Technology*. 59: 6556-6566. DOI: 10.1021/acs.est.5c00080.

Dynamic accounting of carbon uptake in the built environment

Elisabeth Van Roijen [a,1 *], Seth Kane [a], Jin Fan [a], Josefine A. Olsson [a], Baishakhi Bose [b], Thomas P. Hendrickson [c], Sarah L. Nordahl [c], Alissa Kendall [a], Corinne D. Scown [b,c,d,e], Sabbie A. Miller [a]

[a] Department of Civil and Environmental Engineering, University of California, Davis, CA 95616, USA

[b] Biological Systems and Engineering Division, Lawrence Berkeley National Laboratory, Berkeley, CA 94720, USA

[c] Energy Analysis and Environmental Impacts Division, Lawrence Berkeley National Laboratory, Berkeley, CA 94720, USA

[d] Joint BioEnergy Institute, Lawrence Berkeley National Laboratory, Berkeley, CA 94720, USA

[e] Energy and Biosciences Institute, University of California, Berkeley, CA 94720, USA

[*] Corresponding Author: E evanroijen@ucdavis.edu

Abstract:

Transforming building materials from net life-cycle greenhouse gas (GHG) emitters to carbon sinks is key to decarbonizing the industrial sector. Current life-cycle assessments of materials (particularly "low-carbon" materials) often focus on cradle-to-gate emissions, which can exclude fluxes later in the materials' life-cycle. Further, conventional GHG emission characterization disregards the dynamic effects of the timing of emissions and uptake on cumulative radiative forcing from processes like manufacturing, biomass growth, and the decadal carbon storage in long-lived building materials. This work presents a framework to analyze the cradle-to-grave GHG balance of building materials using a time-dependent global warming potential calculation. We apply this framework in the Dynamic accounting of Carbon Uptake in the Built Environment (D-CUBE) tool and examine two case studies: concrete and cross-laminated timber (CLT). When accounting for dynamic effects, the long storage time of biogenic carbon in CLT results in reduced warming, while the slow rate of uptake via carbonation does not result in significant reductions in global warming. The D-CUBE tool allows for consistent comparisons across materials and emissions mitigation strategies at varying life-cycle stages and can be adapted to other materials or systems with different lifespans and applications. The flexibility of D-CUBE and the ability to identify GHG emission hot-spot life-cycle stages will be instrumental in identifying pathways to achieving net-carbon-sequestering building materials.

Graphical Abstract:

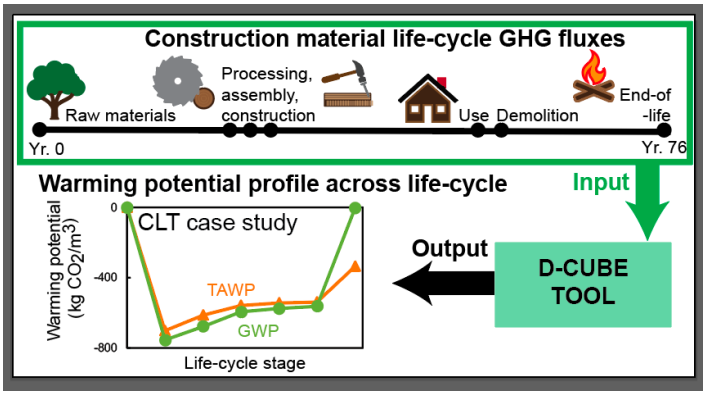

Keywords:

Carbon sequestration, greenhouse gas emissions, materials, time-adjusted warming potential, construction, life-cycle assessment, concrete, cross-laminated timber

Synopsis: Typical global warming potential calculations do not consider the timing of emissions. The presented framework enables assessment of dynamic fluxes of long lifespan materials, more accurately informing decarbonization efforts.

1. Introduction

Buildings and infrastructure are responsible for 40% of United States (US) energy consumption and greenhouse gas (GHG) emissions.[1] To achieve goals of net carbon neutrality by 2050, we need to both reduce these emissions and create carbon-uptake and storage mechanisms, potentially using the built environment as a carbon storage reservoir.[2,3] Numerous permutations of conventional materials have been proposed to store carbon in the built environment, including concrete[3], wood and other biomass,[4] and plastics.[5,6] Such materials can reduce net GHG emissions via their carbon uptake and by replacing higher-emission counterparts.[7,8] Past research on building materials has often focused on cradle-to-gate GHG fluxes.[9] However, meaningful GHG fluxes (i.e., emissions and uptake) can occur later in the material life-cycle (e.g., decomposition at end-of-life (EoL)). Accurate accounting of fluxes at later life-cycle stages is necessary to ensure carbon sequestration on a timescale that is relevant for societal climate change mitigation goals. Cradle-to-gate impacts for building materials have been well studied; however, there is substantial uncertainty in EoL materials management decades in the future, thus consideration of multiple EoL pathways is crucial to determining the range of carbon sequestration outcomes.

Traditional global warming potential (GWP), a methodology derived from the Intergovernmental Panel on Climate Change (IPCC), is calculated assuming that all life-cycle emissions occur at the same time.[10] To determine carbon storage in materials that is relevant for meeting climate change goals, both the quantity and the time period in which these fluxes occur should be addressed. Similar to how acute toxicity (a large dose of a toxin at one time) has a different effect on the human body than chronic toxicity (repeated exposure of smaller doses of toxins), a rapid pulse of GHG emissions has a different impact on cumulative radiative forcing than a slow release of GHG emissions over time. Given the varying timelines for both material production (e.g., tree growth, emissions from energy resources),[11] application of building materials,[4] and their subsequent disposal, the timing of emissions release and uptake can have a significant impact on cumulative radiative forcing and the potential for a material to act as a sequestering resource, but these timing effects are often overlooked for building materials.[12] Dynamic characterization of GHG fluxes more accurately reflects the contribution of emissions in a time-sensitive manner. This methodology has been around for over a decade, with multiple models having been developed with varying approaches. Some models apply discount rates to emissions in the future,[13,14] some account for both the timing of emissions and change in background GHG concentrations over time,[15] and some focus specifically on biogenic carbon fluxes.[16,17] These dynamic warming potential models have been utilized in a variety of applications, such as energy technologies[15,18] and building life-cycles.[19–21] However, a recent review of these various models shows that slight changes in methodologies can have a significant impact on results.[22]

While some excel-based tools for dynamic GHG characterization already exist, such as dynCO2[23], these tools only allow users to examine the total impacts of a product or process, and do not provide a breakdown of emissions based on lifecycle stage. At present, there is a limited understanding of when upfront emissions may be justifiable in exchange for prolonged material use. As a result, many important questions arise when discussing material sustainability and efficient architectural design: When is it justifiable to accept higher emissions at the outset of a product's life cycle if long-term CO2 uptake or a prolonged lifespan can compensate for it? How much carbon sequestration or increased durability would be necessary to effectively counterbalance higher initial emissions? If a material can be engineered to have a significantly lower environmental impact per unit but requires more frequent replacement, what implications does this have for overall sustainability? Additionally, if the ability to influence only one stage of a material's lifecycle exists—due to constraints in the value chain—what is the most impactful intervention that could be made? Possible strategies include prioritizing the use of

repurposed materials, elongating material use, or developing mechanisms to support carbon uptake throughout the material's lifespan. The tool presented herein allows users to examine the dynamic GHG impacts of each lifecycle stage of a product and investigate the possibility of a secondary lifecycle, therefore enabling rapid decision making for sustainable material design.

Another issue that often arises for building materials is how to characterize biogenic carbon. Often times, biogenic carbon is treated as having zero or neutral impacts in life cycle assessments. This approach assumes that the carbon released when biomass is used (e.g., in wood products) is offset by the carbon absorbed during the biomass's growth phase. This simplification can distort the impacts associated with biomass use, partly because of the long growth period of some biomass such as forests, and also because of the long use-phase of materials such as wood in the built environment. To try and improve efforts for tracking carbon, the +1/-1 approach is sometimes applied, which essentially treats biogenic carbon the same as fossil carbon: where any emissions to the atmosphere have a "positive" impact on radiative forcing (i.e., they contribute to climate change), and any CO_2 taken out of the atmosphere has a "negative" impact, offsetting emissions. This method provides a straightforward way to account for carbon flows but fails to consider the timing of when the carbon is released and when it is absorbed. Therefore by applying the +1/-1 approach with dynamic carbon accounting methods, this tool can provide a more accurate understanding of the impacts of bio-based materials in long-term applications.

This tool, the Dynamic accounting of Carbon Uptake in the Built Environment (D-CUBE), utilizes GHG fluxes and the time period of each material life-cycle stage to determine time-sensitive impacts on cumulative radiative forcing, as well as to determine GHG emission hot-spots. Given the multi-decade time horizons for materials in infrastructure applications, emissions are calculated based on time-adjusted warming potentials (TAWPs).[10] While D-CUBE is developed for application to carbon-storing building materials, life-cycle stages that are reflective of other products could replace those presented herein. Next, two case-study applications of the developed framework are provided for an emerging biobased building material, yellow poplar (YP) cross-laminated timber (CLT), alongside a conventional mineral-derived building material, Portland cement concrete. Scenario analysis is performed to examine the effects of factors such as varying production routes and EoL states (e.g., landfilling, combustion, gasification, or pyrolysis for biomass). D-CUBE can be applied to determine the relative contribution of each life-cycle stage to aid in accurately determining material carbon sequestration potential across the entire material life-cycle and to inform production, use, and disposal pathways that can support desired carbon sequestration capacity.

2. Methods

2.1 Developed framework

In this work, we have derived a framework, that pairs a TAWP method, based on work by Kendall [10], with the dynamic GHG fluxes that occur throughout a material's life-cycle and then apply this framework in a developed tool, D-CUBE. Manufacturing emissions and EoL emissions generally occur on very different time scales. For some building materials, carbon can be stored within the material for decadal time horizons. The effects of emissions and removals timing, as well as quantifying benefits of carbon removals shorter than 100 years is of increasing importance as efforts aim to decarbonize the built environment and new materials are engineered to store or utilize carbon. Building from different approaches, including work by Van Roijen et al. (2024)[24] which focuses on time-dependent impacts of concrete carbonation, this framework assembles a unified method for addressing dynamic GHG fluxes

throughout a material's life cycle and allows for modification of end-of-life assumptions and life-cycle time horizons.

2.1.1 Requisite inputs and outputs

To implement D-CUBE, a scope of assessment and inventory of GHG fluxes are needed. While all GHGs can be modeled using this tool, we present an implementation of the method derived in a simplified calculator in the Supporting Information. CO_2, CH_4, and N_2O emissions have been reported as the most prevalent GHG emissions from building materials production,[25] and therefore we focus on these gases. D-CUBE facilitates three primary types of inputs: (1) the CO_2, CH_4, and N_2O emissions (in units of kg/unit product) associated with each life-cycle stage; (2) the CO_2 uptake (kg/unit product) associated with each life-cycle stage; and (3) the duration of specific life-cycle stages (in years), namely raw material acquisition (e.g., rate of photosynthetic carbon uptake in biomass), use/maintenance (e.g., the length of time the product is in service), and EoL (i.e., the time horizon over which end-of-life fluxes are anticipated to occur, such as material decay). It is assumed that manufacturing/assembly, transportation from raw material acquisition to construction, and construction cumulatively occur within one year, and it is assumed that removal/demolition and transportation to waste treatment together occur within one year.

D-CUBE requires several key inputs. First, for the material or product of interest, define a scope of analysis. This scope could include factors such as anticipated shifts in material use (e.g., demand for repair), potential EoL management pathways, and the expected time horizons for material synthesis, use, and EoL. Further, scenario analyses could be outlined that consider future changes in energy grids, material availability, and alternative production pathways (e.g., using carbon capture and storage for energy facilities, and use of renewable energy resources). We outline these key phases to consider while determining the scope of assessment in Figure 1. After defining a scope, the practitioner must address anticipated GHG uptake and emissions at each of the eight primary stages presented in Figure 1. Namely, an inventory of the CO_2, CH_4, and N_2O emissions and uptake must be determined per unit of material. These GHG fluxes must also be quantified for any permutations of interest (e.g., electricity grid mix variations). With these inputs and outputs, the methodology can be implemented (as discussed in the subsequent sections).

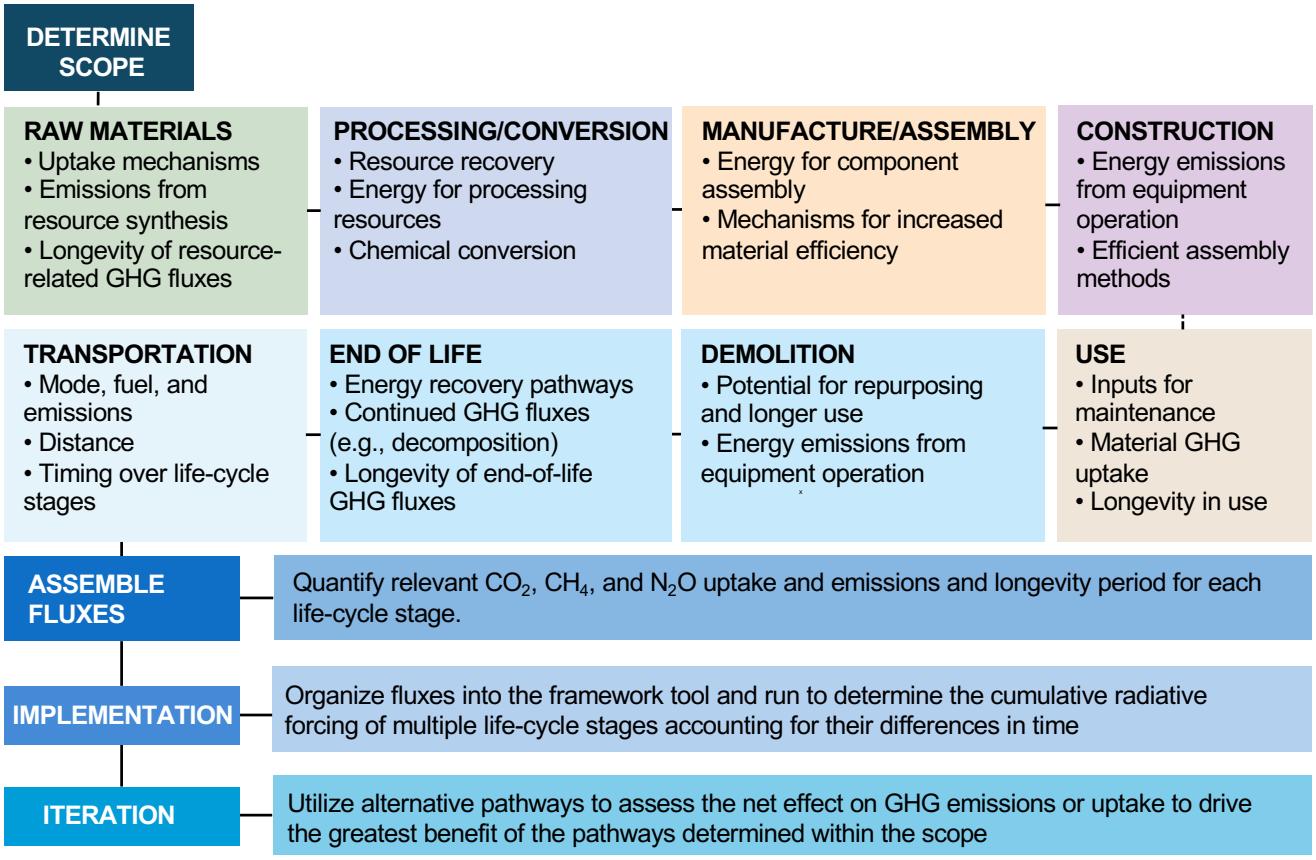

Figure 1. Data considerations to determine for the scope of assessment, greenhouse gas fluxes to consider, implementation, and iteration for the proposed method. (Note: only example parameters are listed, additional parameters may exist)

The outputs of D-CUBE provide mechanisms to assess the cradle-to-grave life-cycle time-adjusted global warming effects for a building material. The case studies are presented in terms of 1 m^3 of product; however, the calculation approach described is inherently functional unit independent. More complex material systems can be modeled if input fluxes are normalized to that specific system, as the method is agnostic to product type. Results output a traditional GWP value as well as a TAWP value. The TAWP value considers the impact of the timing of emissions and the resulting impact on cumulative radiative forcing. In addition, D-CUBE provides the percent contributions of each life-cycle stage (i.e., resources, processing, manufacturing, construction, use, demolition, end-of-life, and cumulative transportation-related emissions throughout the system) to the overall TAWP. This breakdown allows users to determine hot-spots of uptake and sequestration, and as a result, they can alter parameters to understand manufacturing, use, and disposal pathways that drive desired net fluxes. For the D-CUBE outputs, note that if the overall TAWP is negative, then any life-cycle stages with positive emissions will have a "negative" percent contribution, and any life-cycle stages that have negative emissions (emissions uptake), will have a "positive" percent contribution, and *vice versa* (See Supporting Information). In addition, the relative contribution of each GHG (CO_2, CH_4, and N_2O) flux in each life-cycle stage is presented. Both traditional GWP and TAWP are calculated with a 100-year time horizon using data from the Intergovernmental Panel on Climate Change's (IPCC's) AR5 report.[26]

2.1.2 TAWP calculation

The impacts due to radiative forcing of a specific GHG are dependent on the year at which the flux (i.e., emissions or uptake) occurs and the magnitude of that flux, as seen in Equations 1 and 2 below. We

assess net emissions associated with a product as a function of the inventory of fluxes and the TAWP to capture the radiative forcing from those fluxes as follows:

$$Net\ GHG\ emissions = \sum\left(Q_{i,y} \times TAWP_{i,y}\right) \quad \text{Eq 1.}$$

Where Q is the quantity of GHG emissions or uptake, y is the year of emission (where $y = 0$ at the beginning of the analytical period), i is the type of GHG emission (here focusing on CO_2, CH_4 and N_2O), and TAWP is the time-adjusted warming potential for an emission of gas i, in year y. To allow for comparisons with conventional GWP characterization factors, Equation 1 is also implemented with the IPCC's AR5 GWP 100 factors.[26] In this permutation, the GWP characterization factors for each GHG are used to replace the TAWP factors.

To determine an appropriate TAWP, cumulative radiative forcing is assessed by calculating the integral of radiative forcing over a given time horizon. The timing of emissions is captured by the variable y, as defined by equation 1. By subtracting y from the time horizon, the time horizon for integration of radiative forcing is more accurately captured than with a traditional GWP factor.[10]

$$TAWP_i = \frac{\int_0^{AT-y} RF_i}{\int_0^{AT-y} RF_{CO2}} \quad \text{Eq 2.}$$

In Equation 2, RF_i and RF_{CO2} refer to the radiative forcing of GHG i and CO_2, respectively. These calculations are based on background GHG concentrations reported in IPCC AR5, and do not reflect changes of background GHG concentrations in the future. AT refers to the analytical time horizon. In the case studies presented herein, a time horizon of 100 years is utilized to draw comparisons to traditional GWP results. By using a 100-year time horizon, the analytical period for cumulative radiative forcing is truncated at 100 years from the beginning of the analytical period. For example, if an emission occurs at year 20, then only 80 years of cumulative radiative forcing will be accounted for. Figure 2 illustrates how the impacts of emissions for a typical building might be considered using various time horizons.

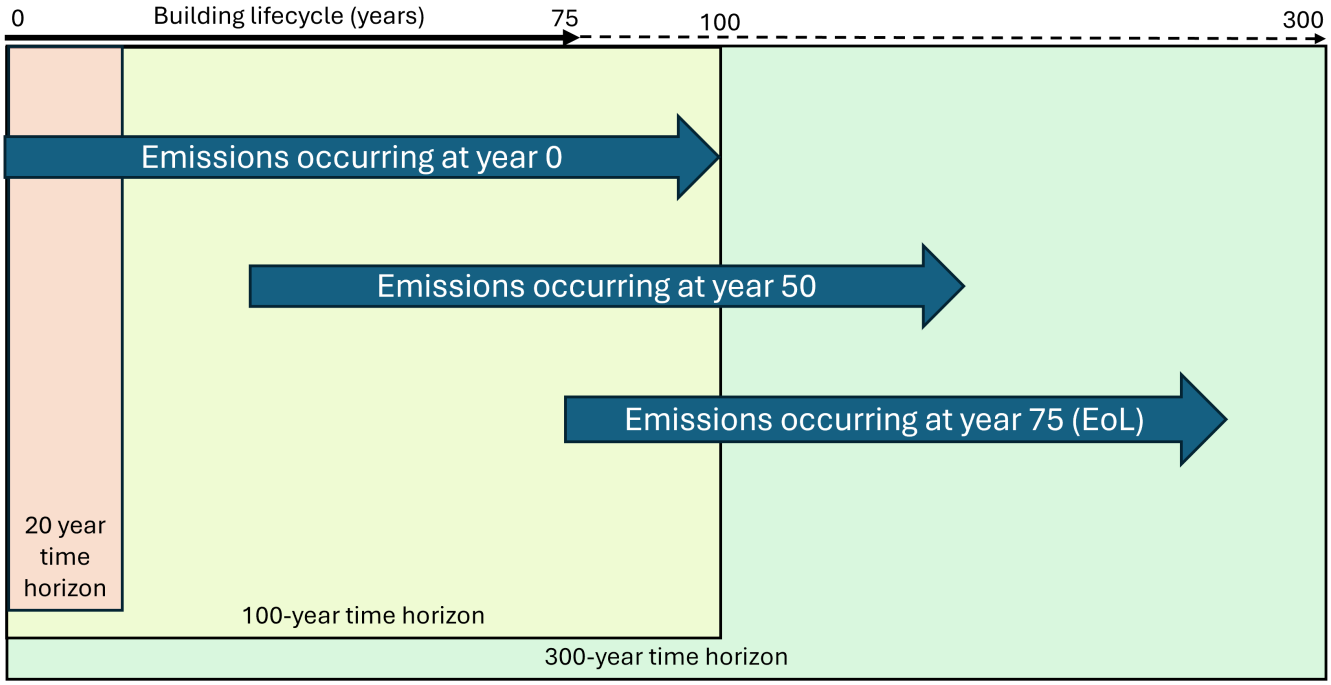

Figure 2. Qualitative representation of the impact of a chosen analytical time horizon on resulting greenhouse gas characterization using TAWP. An example of a 20-, 100- and 300-year time horizon is shown in orange, yellow and green respectively. Navy blue arrows depict the lifetime of a hypothetical greenhouse gas. Note that the atmospheric lifetime of different greenhouse gases varies by type.

Using a longer analytical time horizon for integration of radiative forcing will capture more of the warming effects of emissions, especially those with longer atmospheric lifetimes, it can also result in undervaluing the immediate impacts of shorter-lived GHG emissions such as CH_4. This phenomenon has been well documented, and it has led to much debate regarding the appropriate method for selecting an analytical time horizon. It is also important to note that under longer time horizons, the difference in results between static and dynamic GHG characterization methods will be less pronounced. For example, Kendall et al. show that under a 100-year time horizon, dynamic GHG characterization results in 30% lower impacts on global warming for a commercial building lifecycle, while under a 500-year time horizon it is only 5% different[27] . Given the importance and sensitivity of the time horizon on the results, D-CUBE allows users to select a time horizon of 20, 30, 50, 100, 300 or 500 years to analyze the appropriate time horizon for their work or to examine the change in results between time horizons.

2.1.3 Use and assessment

The outputs of D-CUBE can be used to drive materials, products, and systems engineering. For those desiring to develop materials that can act as a CO_2 reservoir and store either atmospheric CO_2 or CO_2 captured from flue gas, thus bypassing the need for geological reserves, this method can capture the decadal benefits of potential temporary and long-term storage that are not captured with GWP characterization factors. Maximum storage potential for any given material will depend on the chemical composition of the material, manufacturing methods, potential in-use longevity, and disposal pathways. Yet, D-CUBE facilitates an understanding of guiding principles to target alternative measures throughout the material's life-cycle that would increase net-uptake and sequestration potential. As would be expected, at any life-cycle stage, minimizing GHG emissions and maximizing CO_2 uptake will drive down net fluxes and increase net storage potential. However, depending on the magnitude of uptake versus emissions, the longevity of different life-cycle stages will have varying effects. To drive

maximum carbon uptake and storage, typically, elongating periods where CO_2 is stored and accelerating the rate for which a certain quantity of CO_2 is removed from the atmosphere are desirable.

By implementing this tool, users can systematically quantify the benefits of various decarbonization strategies for the built environment. These can include factors such as tradeoffs between high emissions upfront and longer lifespan (potentially reducing maintenance, repair, or replacement), which is a common debate in engineering long-lived infrastructure materials.[28–30] Herein, the effects of how prolonging carbon storage or reducing replacement-related emissions compared to a pulse of emissions at the onset through material production can be quantified. Further, the influence of varying future decarbonization of energy resources, varying future resource inputs, and varying future waste management on the efficacy of materials acting as carbon storage can be assessed. By varying inputs, stages of the life-cycle that have the greatest effect on net fluxes, and thus should be optimized to drive desired emissions profiles for the material, can be determined through sensitivity analyses.

2.2 Data considerations for greenhouse gas fluxes

Assessment of TAWPs should consider timing, type, and magnitude of GHG emissions throughout the life-cycle of a material or product. During raw material formation and extraction, uptake in mineral materials primarily occurs at geological time scales that do not contribute to relevant CO_2 removal and storage,[31] and in photosynthetic biogenic materials, uptake occurs at annual (agricultural crops) or decadal (forestry) time scales.[32] Emissions occur from both mineral and biogenic materials due to energy use during extraction or harvesting,[33] as well as from other emissions sources, such as those associated with fertilizer use and land management.[34,35] During material processing, conversion, manufacture, assembly, and construction life-cycle stages, emissions are dominated by energy use as well as chemical reactions during processing (e.g., cement production [36,37]). During the use phase, some materials, such as concrete, are capable of certain degrees of CO_2 uptake during use under the appropriate exposure conditions.[38] Notably, this life-cycle stage also defines how long the material's lifespan is, during which, if there is bound carbon, the in-use material may act as a temporary GHG reservoir. At EoL, emissions associated with energy use for demolition and material processing should be considered, and some EoL pathways may result in emissions due to material decomposition (e.g., combustion of biomass). The EoL for a material may occur decades after production, with common practices varying by material type and locally available waste management infrastructure, making the EoL scenario highly uncertain. Therefore, it is advantageous to consider multiple EoL pathways to assess the effects of dynamic GHG fluxes of various potential pathways. Transportation may occur between and during all stages described above, resulting in GHG emissions. Additional GHG fluxes may occur due to material waste during all stages prior to use or during transportation. Waste can result from factors such as over-ordering, damage during handling or storage, and incorrect installation, and this waste drives increased material production and associated GHG fluxes.[39] See Supporting Information Section 2.4 for a complete description of fluxes at each life-cycle stage.

In the D-CUBE tool, a user should consider shifts driven by material performance and durability if applicable to the scenarios being considered. As D-CUBE is independent of the functional unit (GHG fluxes can be normalized to any unit of material), it can easily be adapted to functional units that consider these critical performance metrics and, therefore, their associated GHG fluxes. D-CUBE follows the life-cycle of an individual material, so if material replacement or maintenance is necessary during the use phase of the whole system, additional material production would be required, which may vary in timeline to the original material. If a loss in material performance influences emissions tied to other systems (e.g., an increase in thermal conductivity with time, leading to greater HVAC system requirements), those additional emissions can be modeled at the user's discretion.

The D-CUBE model assumes linear carbon uptake within each life cycle stage, which simplifies the non-linear growth dynamics of biomass (e.g., trees or agricultural residues). While this approach does not capture the details carbon flux within each stage, the effect on the final TAWP is typically minor, as the total carbon content at the end of each stage remains the same. This simplification ensures the model remains practical and easy to use, but users should be aware of this limitation when interpreting the results.

2.3 Case study application

In this section, we exemplify the implementation of D-CUBE through two case studies to provide context for framework implementation. These case studies compare D-CUBE results to conventional GWP characterization factor-based assessments. Here, we assess the GHG fluxes associated with each life-cycle stage of Portland cement concrete and CLT. Concrete was selected due to its ubiquity as the most widely used building material, and it represents a class of mineral-based building materials. This choice also facilitates comparisons with findings from existing literature. CLT, another commonly used building material, is a biogenic-based material that demonstrates superior mechanical performance compared to other wood-based materials like glulam and plywood. Furthermore, CLT has the potential for use in mid- to high-rise construction, positioning it as a viable alternative to conventional materials like concrete. Here, we consider CLT made with YP. We aim to highlight the carbon sequestration potential of these materials and assess how they are affected by varying parameters such as energy systems, in-use lifespans, EoL scenarios, and material processing.

A functional unit of 1 m^3 of material is used for this assessment. In both cases, emissions associated with maintenance in the use-phase and transportation emissions are excluded, given the high uncertainty in maintenance depending on spatiotemporal drivers (e.g., susceptible to extreme weather events or not) and the high variability in transportation distances, which are specific to a particular facility and location. A 50-year service life is assumed for the baseline scenario for both concrete and CLT (Figure 3) and a 21-year growth period for biomass growth.

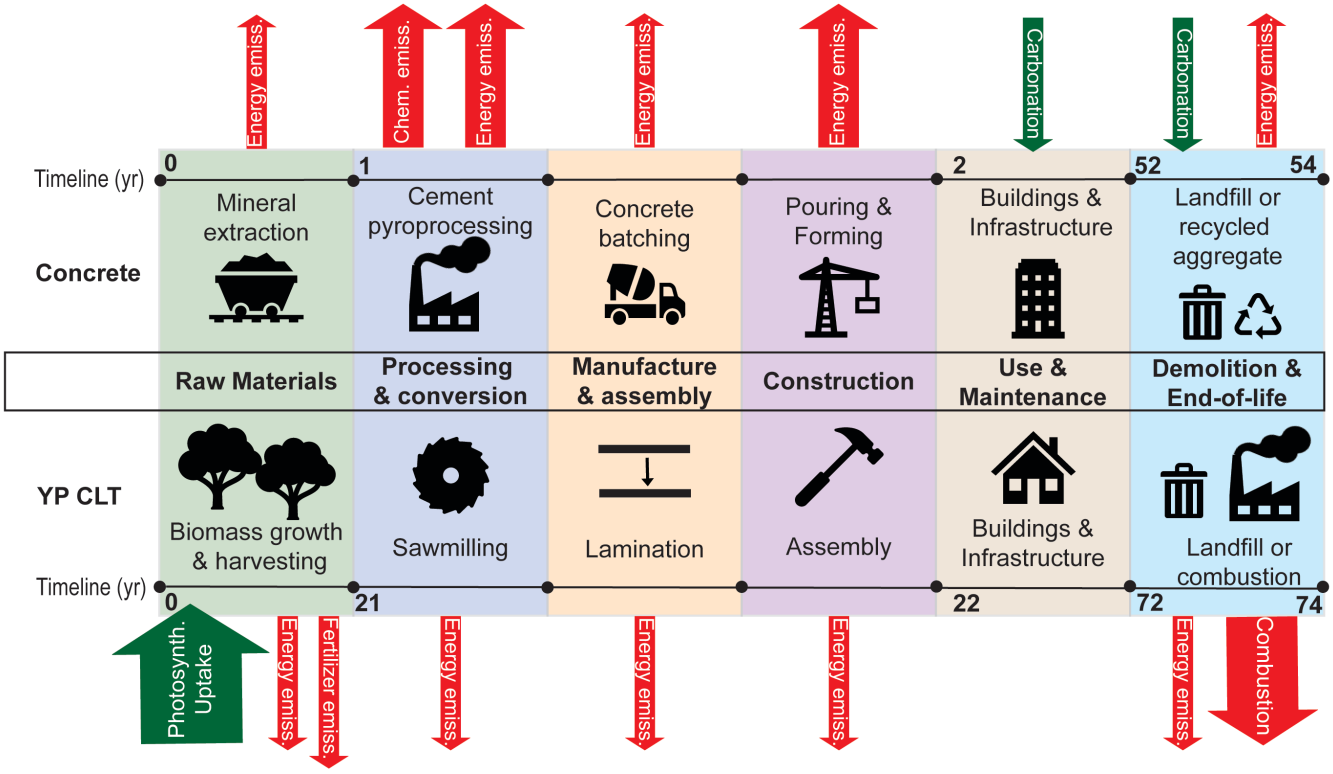

Figure 3. Life-cycle stages for Portland cement concrete and yellow poplar (YP) cross-laminated timber (CLT), showing the length of time and primary sources of carbon fluxes for each life-cycle stage (See Supplemental Table 1 and 2 for complete flux sourcing). Arrow sizes approximate the proportional magnitude of emissions.

2.3.1 Baseline modeling assumptions to quantify GHG fluxes

For concrete, the inventory modeling assumptions and data sources included inputs from raw material acquisition through concrete disposal at the end of a service life within a building (Table S1). For the baseline case, a Portland cement concrete mixture is modeled, in which there are no supplementary cementitious materials (SCMs) considered, and the compressive strength at 28-days is 25 MPa.[40] The GHG emissions from raw materials extraction, processing and manufacturing of cement were determined using the OpenConcrete LCA tool by Kim *et al.* (2022)[41]. Carbon uptake occurring during the use-phase and end-of-life stages as a result of carbonation are modelled based on results from Van Roijen *et al*. (2024).[24] Further, the GHG emissions generated during the construction and demolition phases were based on Guggemos *et al*. (2005) [42]. See Supporting Information for a detailed description of modelling assumptions and data sources (Table S1 and Section 3.1).

For the YP CLT, the inventory modeling assumptions and data sources included inputs from raw material acquisition (in this case, YP cultivation and harvest) through disposal (modeled based on an assumption of combustion with energy recovery, see Supporting Information Table S2 and Section 3.2). The acquisition of the biogenic YP included aspects such as growing and logging operations. It was assumed that YP was harvested after 21 years of growth[32] using shelterwood harvesting. Only aboveground biomass was considered in this study and the GHG fluxes do not include long-term changes in soil carbon stocks, as these are highly uncertain and dependent on the land use history, local soil type, and climate. To address bound carbon resulting from photosynthesis during cultivation, a carbon content of 50 wt.% of total wood was used to quantify the CO_2 uptake during biomass growth.[43]

These long-duration uptake flows were paired with a pulse of emissions from the extraction of materials processing (saw mill operations) and manufacturing (e.g., kiln drying and CLT production).[44] Unlike the concrete case, CLT does not take up CO_2 during the use phase. Therefore, because we exclude impacts from maintenance and repair in these models, no emissions or uptake is considered in the use phase for CLT structures. The baseline model assumes direct combustion of the YP CLT at its EoL.[45]

2.3.2 Greenhouse gas improvement scenarios

As part of this work, we also aim to present a proof of concept of theoretical maxima of sequestration of materials. As noted earlier, the maximum uptake a material can offer will depend on GHG fluxes and duration due to composition, manufacturing methods, installation, use, and disposal pathways. To present a proof of concept as to how this framework can be implemented to understand potential maximum sequestration, we hold several parameters constant and investigate the influence of others on driving down cumulative radiative forcing. In a full scenario analysis, all potential permutations could be considered (e.g., varying chemical composition, improving manufacturing efficiency, fuel switching, prolonging in-use, and EoL carbon storage). For all decarbonized energy grid scenarios, we include decarbonization of the electricity grid (i.e., no GHG emissions from electricity) and use of natural gas as opposed more carbon-intense fuels (e.g., coal) for any thermal energy sources used in material processes. Emissions from chemicals in the harvest stage of CLT were also considered to be negligible in those scenarios, assuming that more environmentally friendly sources were to be used to replace the herbicide and lubricant in CLT harvest process.

For concrete, seven mitigation scenarios are considered to investigate the impact on overall life-cycle emissions to demonstrate how strategies for altering material production and disposal could inform the pathway leading to maximum uptake. These seven scenarios were: (1) decarbonized energy grid, (2) 20% substitution of cement with fly ash, (3) 50% substitution of cement with ground granulated blast furnace slag, (4) landfilling of concrete at EoL, (5) extending the use-phase of concrete to 80 years, (6) extending the end-of-life stage of concrete to 5 years, and (7) combining a decarbonized energy grid, an extended use phase, and 20% replacement of cement with fly ash. The decarbonized electricity grid was assumed to generate zero emissions, and no allocation of emissions from the generation of industrial by-products used to substitute cement were considered (fly ash and the blast furnace slag). Specific conditions were considered for the concrete use phase and EoL exposures to capture the effects of carbonation. It was assumed the concrete was exposed in an urban environment (reflective of CO_2 concentration) without coatings during the use phase. It was also assumed that carbonation during the EoL phase happens in an exposed, industrial environment where the demolished concrete is crushed to small (1-40mm) pieces and carbonated for 1 year, with carbonation based on [24]. In the landfill scenario, the concrete is assumed to be crushed to coarse (100-500mm) pieces. See Supporting Information for detailed assumptions for each scenario.

For the CLT, five mitigation scenarios were considered, primarily focusing on the influence of EoL management. The baseline scenario used herein is direct combustion at a power plant with the baseline energy grid. The following mitigation scenarios at EoL were assessed: (1) gasification (baseline energy grid), (2) slow pyrolysis (baseline energy grid), (3) direct combustion (decarbonized energy grid), (4) gasification (decarbonized energy grid), and (5) slow pyrolysis (decarbonized energy grid). For the scenarios with decarbonized electricity grid, the emissions from raw materials stage to demolition stage were assumed to be zero, and carbon uptake in the biomass growth period and emissions from combustion were considered. The GHG fluxes for these different pathways remain the same from the raw material acquisition phase up to demolition. For the pathways that produce biochar (e.g., slow pyrolysis), no carbon fluxes from life-cycle stages after the production of biochar (e.g., avoided

emissions from the agricultural application or material replacement or emissions from biochar degradation) were included. For example, this considers the utilization of the char for a second life, where the carbon that remains bound can be stored for the longevity of another building application (e.g., in a concrete mixture). The heating value of the bio-oil was compared to that of petroleum fuels to determine the emissions tradeoff for an equivalent amount of heat. For example, if the bio-oil was to be blended in very small quantities and co-processed with crude oil, then it could offer a partial replacement to the fossil oil.[46] We did not consider the transportation or processing for these subsequent use phases. The variations in emissions only occur at the EoL stage to show a proof of concept. Emissions from the biomass power plant were taken into account,[47] and the generated electricity was compared to average emissions from the national power grid to determine the emissions tradeoff for an equivalent amount of generated electricity. Electricity generation efficiencies for different biomass power plants were sourced from the literature, resulting in varied efficiency rates across the three pathways. See Supporting Information for detailed assumptions and modeling details for each scenario.

3. Results

A synthesis of emissions outputs by life-cycle stage, both with the use of GWP characterization factors and with the use of TAWPs are presented in Figure 4a for the baseline cases of 1 m^3 concrete and CLT.

In the baseline case for concrete, if conventional GWP100 characterization factors are applied (as are conventionally used in reports such as Environmental Product Declarations), the cumulative life-cycle GHG emissions are 334 kg CO_2e /m^3. As expected, most emissions are generated during the processing phase (e.g., calcination, thermal energy for cement production). The construction phase is the second largest contributor, contributing 28% of the total GHG emissions. While carbonation of concrete is gaining attention as a potential direct air capture mechanism,[3,48] the CO_2 uptake during the use phase and at EoL resulting from concrete carbonation is small compared to the total GHG emissions. When TAWPs are considered, the total life-cycle emissions become 98.5% (330 kg CO_2e/m^3) of the GHG emissions when TAWPs are not considered. In this baseline case, the TAWP and GWP methodologies result in similar life-cycle emissions due to most emissions occurring within the first few years. However, the TAWP method used in the D-CUBE tool results in a slightly lower overall life-cycle warming potential due to the reduced impact of emissions occurring in later stages (i.e., emissions from construction and demolition).

Unlike concrete, CLT life-cycle GHG fluxes result in a net-uptake due to the large quantity of atmospheric CO_2 that is taken in during biomass growth (Figure 4a). For CLT, most GHG emissions are generated at the EoL phase from combustion. When accounting for the dynamic effects of GHG fluxes via TAWPs, CLT results in sequestration of -334 kg CO_2e /m^3 over the life-cycle. However, when GWP100 characterization factors are used, net life-cycle GHG fluxes are near net-zero. These near net-zero emissions when using GWP are a result of later life-cycle stages (e.g., construction, disposal), resulting in GHG emissions that counteract the uptake during biomass cultivation. However, when the dynamic effects of early CO_2 uptake and carbon storage during use are considered relative to periods in which GHG emissions occur with TAWPs, the beneficial effects of CLT on CRF becomes apparent.

Previous LCAs of CLT focused on cradle-to-gate (i.e., harvesting through manufacturing) emissions of CLT, ranging from about 80-200 kg CO_2e/m^3 CLT.[49,50] Excluding sequestration and post-manufacturing stages, our findings are similar (185 kg CO2e/m^3), but results can vary based on lumber source, processing and manufacturing energy demands, electricity grid mix, and other supply chain characteristics.

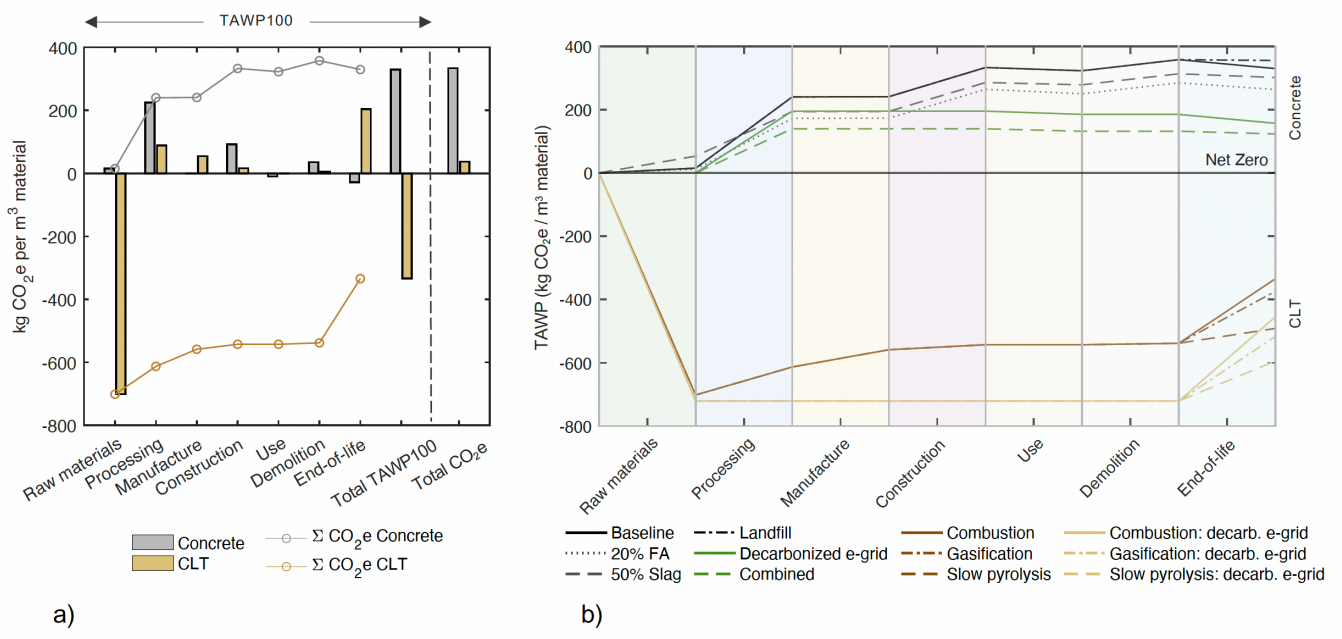

Figure 4. (a) Total emissions by life-cycle stage (bars) and net emissions per life-cycle stage for the baseline concrete and CLT scenarios ("Total CO_2e" represents the implementation of GWP 100a characterization factors to assess cumulative emissions throughout the life-cycle). (b) Life-cycle GHG emissions (in terms of TAWP) for concrete and CLT under various mitigation scenarios. Decarb. e-grid = decarbonized energy grid.

3.1 Improving sequestration potential

For concrete, the GHG emissions notably exceed the CO_2 uptake. However, specific interventions can result in higher uptake and lower emissions over the life-cycle. Of the scenarios considered, the greatest reduction in life-cycle emissions was achieved by decarbonizing the energy grid and using low-carbon fuels in cement production. [] This decarbonization strategy resulted in negligible GHG emissions during the use and end-of-life phases, allowing the carbonation at these stages to support a small net-CO_2 uptake. As shown in Figure 4b, a greater reduction in GHG emissions but a similar quantity of CO_2 uptake from carbonation was achieved with the "Combined" scenario, where cement substitution by SCMs (20% fly ash), an extended service life (80 years as opposed to 50 years), and decarbonized energy grid and low carbon fuels are considered. The "Combined" scenario leads to 123 and 93 kg CO_2e per m^3 concrete over the complete life-cycle, using TAWPs and traditional GWPs, respectively.

In the scenarios for concrete in which a zero-emissions energy grid and low-carbon fuels are considered, the TAWP results are higher than when GWP characterization factors are used (see Supporting Information Figure S1). This is because no GHG emissions are occurring during the construction and demolition phases, which, in the baseline scenario, outweigh the quantity of carbon uptake from carbonation. As a result, all emissions occur during the first year, and therefore, the climate benefits of the carbon uptake, are much smaller when accounting for the long-time horizon over which they occur. When the dynamic effects of how much later this uptake is occurring are considered, they are not as beneficial as GWP characterization factors would suggest. Extending the end-of-life phase from 1 to 5 years and reducing the diameter of the demolished concrete particles has a minor effect on the sequestration potential for concrete in this case.

Given that the EoL emissions for CLT contribute the most to overall life-cycle emissions, various EoL pathways were considered (Figure 4b). The life-cycle GWPs per m^3 CLT when assuming combustion, gasification, and slow pyrolysis as EoL scenarios are 37 kg, -70 kg, and -417 kg CO_2e, respectively, while the TAWP values are -334 kg, -374 kg, and -491 kg CO_2e, respectively. Regardless of the EoL scenario examined, near-zero or negative life-cycle emissions were achieved using both GWP and time-adjusted methods. This trend is primarily due to the photosynthesis of biomass during growth, which absorbs 3.8 and 4.3 times the amount of GHGs associated with raw material acquisition, processing, manufacture, construction, and demolition combined for GWP and the dynamic method used herein, respectively. Notably, greater net benefits to cumulative radiative forcing were found when considering the dynamic effects of these fluxes. This shift is due to the CLT acting as a temporary carbon pool during the 50-year use phase, which delays the EoL GHG emissions and thereby reduces the impact on cumulative radiative forcing during the analytical time horizon. This dynamic benefit of temporarily storing carbon is not reflected by GWP characterization factors. Further, at the EoL stage, carbon in the biomass is partially stored in the ash (combustion) or char (gasification and pyrolysis), while the rest is emitted via oxidation. For example, the carbon emission from decay and combustion comprised 97.3% of the total carbon in the biomass. The TAWP result for the gasification scenario is 40 kg CO_2e lower than that of direct combustion, attributable to the increased yield of solid-phase materials (char) that sequester more carbon.

Similarly, slow pyrolysis exhibits a 47% lower TAWP result compared to combustion due to a higher char yield. However, the energy generated from biomass through combustion can replace conventional energy sources and their associated GHG emissions. As such, we still see reduced TAWP from combustion even though most of the carbon was released. The emissions benefits from displacing electricity and energy from the grid may be reduced when cleaner energy (i.e., via a decarbonized energy grid) is being substituted. However, the overall TAWP was 36% lower in the combustion scenario when a decarbonized energy grid was used due to the elimination of energy-derived GHG emissions from the raw materials stage to the removal stage. Notably, a landfilling scenario for CLT shows high spatial variability in emissions and uncertainty in future landfilling practices.[51] If landfilling were considered, emissions would occur over a time period of greater than a year, be highly spatially variable, and a larger fraction of emissions would be in the form of methane rather than CO_2, depending on exact landfilling practices and methane capture. Our analysis of the landfill scenario, which assumes EoL emissions (based on [52]) occur over 10 years and all other life-cycle stages emissions/uptake are the same as the baseline (combustion) scenario, indicated that the GWP and TAWP were 349 kg CO_2e and -277 kg CO_2e, respectively. Additionally, material reuse or recycling is an important EoL pathway for CLT, with ease of reuse being often touted as a key benefit of CLT over other wood products.[53] Consideration of second life and beyond emissions would provide key insight into the role of avoided emissions and dynamic warming effects in the circular economy broadly. The CLT recycling scenario, which assumes a 20-year secondary use-phase, the same emissions from construction and demolition as in the first use-phase, and combustion at EoL, resulted in reduced TAWP (-509 kg CO_2e) compared to combustion without recycling (-334 kg CO_2e) due to delayed GHG emissions after recycling. The rotation cycle varies among wood products. As such, a sensitivity analysis of the rotation cycle of the CLT, considering 17 years and 25 years of growth period of the YP, was conducted. Results showed only -6% and 5% differences in terms of TAWP compared to that of the 21-year combustion scenario. We note, however, that care should be taken to consider uncertainty (e.g., in potential ranges of energy grid decarbonization) in future avoided emissions from material replacement with recycled material to accurately reflect the range of emissions reduction possible with future reuse and recycling scenarios.

Our analysis of the concrete and timber case studies revealed similar patterns in life-cycle GHG flux, aligning with trends observed in existing literature. This finding underscores the dynamic differences in GHG characterization between GWP and TAWP. In some cases, CO_2 uptake through concrete carbonation is regarded as having a notable influence on the decarbonization of cement and concrete.[54–56] However, in the concrete scenario presented here, GHG emissions exhibited minimal variation across life-cycle stages, as they are predominantly concentrated in the early stages of the analyzed time horizon.[57] A previous study comparing CO_2 uptake scenarios with decarbonization strategies found similar results, indicating that CO_2 uptake during service life has a minor impact on GWP. In contrast, the use of SCMs and alternative fuels offers the greatest potential for reducing life-cycle CO_2 emissions, unless the concrete is crushed at EoL to carbonate over decades.[58] In contrast, the carbon uptake by biomass and its delayed release during energy generation affects the atmospheric CO_2 balance, leading to significant differences between GWP and TAWP.[59–61] This is consistent with the findings of Ericsson et al. (2013)[62], who demonstrated that the timing of carbon fluxes in bioenergy systems, such as short-rotation coppice willow, plays a critical role in determining their climate impact. Unlike conventional LCA, which omits these temporal dynamics, our D-CUBE model incorporates the CO_2e flux over time allowing for identification of the most effective strategies for reducing emissions and achieving near-zero emissions or net-carbon-storage goals.

4. Discussion

By breaking down emissions by life-cycle stage, as well as examining the impact of the timing of emissions on cumulative radiative forcing, this tool allows for a robust understanding of current hot spots in the life-cycle of materials or processes. Furthermore, it allows for comparisons of various scenarios using consistent methodologies, which can help enable material developers, policymakers, and other stakeholders to investigate pathways toward reducing GHG emissions and drive maximum sequestration in the built environment. This calculation method offers a reliable method for evaluating the warming potential of novel construction materials, which in turn aids in identifying potential sustainable materials and construction strategies.

In this work, we see that accounting for the timing of GHG emissions release and uptake is especially important for materials and processes that have considerable GHG fluxes and storage capacity spanning over a long-time horizon (e.g., decadal use of building materials). In the case of CLT, we see that EoL strategies that allow for greater quantities of carbon sequestration, such as gasification and slow pyrolysis, result in significantly lower life-cycle GHG emissions than processes that result in CO_2 release, such as combustion. For concrete, we see that production-related mitigation strategies (such as decarbonizing energy sources and implementing SCMs) have a larger impact on life-cycle emissions than end-of-life strategies, such as concrete crushing during demolition.

To properly assess potential mitigation strategies, it is important to consider environmental and human health impacts outside of GHG emissions, such as particulate matter emissions, eutrophication, ecotoxicity, and biodiversity loss. Therefore, future work can expand upon this tool to consider more inputs than just GHG emissions. Furthermore, the current tool does not allow for a detailed understanding of the timing of emissions occurring within a multi-year life-cycle stage, such as maintenance occurring during use. Rather, it uses an assumption that the emissions occur at a consistent rate throughout the time period of the life-cycle stage. Therefore, future work could expand upon this tool, to generate a more accurate understanding of the emissions occurring during long life-cycle stages. Further, the authors note that future climate changes can influence the representativeness of the warming potentials used in this tool, hence, to reflect potential changes, the GWPs should be continuously updated based on values reported by IPCC. In this study, scenario analyses were performed to understand the impact of different end-of-life assumptions on the lifecycle impacts of concrete and CLT. In addition to performing a scenario analysis, it is also important to understand the inherent uncertainty

associated with the emissions fluxes of each lifecycle stage, which is not a built-in capability of this tool. Therefore, future work should expand upon this tool to enable robust uncertainty analyses.

D-CUBE is a straightforward yet powerful tool for assessing the climate impacts of long-lived products, such as buildings. Unlike static methods with fixed time horizons, D-CUBE enables a comprehensive, time-sensitive comparison that highlights critical design choices, including the selection of different time horizons and end-of-life options, including re-use and recycling, in decision-making. This capability is especially valuable in supporting informed decisions in response to the climate change challenge. Additionally, by requiring only inputs of life-cycle stage timing and emissions by GHG type, this tool aims to reduce the data requirements of dynamic GHG accounting, by performing dynamic characterization calculations in the background, making application and meta-analysis of dynamic warming effects more accessible to LCA practitioners, material developers, policymakers, and other stakeholders.

[1] Present Address: National Renewable Energy Laboratory, Golden, CO, 80401, USA

Supporting Information. Detailed description of how to use the D-CUBE tool and further information regarding case study methods and assumptions. Excel file with D-CUBE tool.

Acknowledgements

S.K., J.F., B.B., T.H., C.D.S., and S.M.'s contribution to this work was funded through the US Department of Energy, Advanced Research Projects Agency–Energy (ARPA-E, Grant #DE-AR0001625). J.O., E.V.R.'s contribution to this work was funded through the US National Science Foundation (NSF, Grant #CBET- 2143981). This article represents the views of the authors, not necessarily those of the funder. This work was supported in part by the U.S. Department of Energy, Office of Science, Office of Biological and Environmental Research, through contract DE-AC02-05CH11231 between Lawrence Berkeley National Laboratory and the U.S. Department of Energy. The U.S. Government retains and the publisher, by accepting the article for publication, acknowledges that the U.S. Government retains a nonexclusive, paid-up, irrevocable, worldwide license to publish or reproduce the published form of this manuscript, or allow others to do so, for U.S. Government purposes.

Declaration of interests

C.D.S. has a financial interest in Cyklos Materials.

References

(1) National Academies of Sciences, Engineering, and Medicine. *Gaseous Carbon Waste Streams Utilization: Status and Research Needs*; National Academies Press: Washington, D.C., 2019; p 25232. https://doi.org/10.17226/25232.

(2) Miller, S. A.; Van Roijen, E.; Cunningham, P. R.; Kim, A. Opportunities and Challenges for Engineering Construction Materials as Carbon Sinks. *RILEM Technical Letters* **2021**, *6*, 105–118. https://doi.org/10.21809/rilemtechlett.2021.146.

(3) Cao, Z.; Myers, R. J.; Lupton, R. C.; Duan, H.; Sacchi, R.; Zhou, N.; Reed Miller, T.; Cullen, J. M.; Ge, Q.; Liu, G. The Sponge Effect and Carbon Emission Mitigation Potentials of the Global Cement Cycle. *Nature Communications* **2020**, *11* (1), 1–9. https://doi.org/10.1038/s41467-020-17583-w.

(4) Churkina, G.; Organschi, A.; Reyer, C. P. O.; Ruff, A.; Vinke, K.; Liu, Z.; Reck, B. K.; Graedel, T. E.; Schellnhuber, H. J. Buildings as a Global Carbon Sink. *Nature Sustainability* **2020**, *3* (4), 269–276. https://doi.org/10.1038/s41893-019-0462-4.
(5) Meys, R.; Bachmann, M.; Winter, B.; Zibunas, C.; Suh, S. Achieving Net-Zero Greenhosue Gas Emission Plastics by a Circular Carbon Economy. **2021**, *76* (October), 71–76.
(6) Stegmann, P.; Daioglou, V.; Londo, M.; Vuuren, D. P. Van. Plastic Futures and Their CO 2 Emissions. **2022**, *612* (December). https://doi.org/10.1038/s41586-022-05422-5.
(7) Röck, M.; Saade, M. R. M.; Balouktsi, M.; Rasmussen, F. N.; Birgisdottir, H.; Frischknecht, R.; Habert, G.; Lützkendorf, T.; Passer, A. Embodied GHG Emissions of Buildings – The Hidden Challenge for Effective Climate Change Mitigation. *Applied Energy* **2020**, *258* (June 2019), 114107. https://doi.org/10.1016/j.apenergy.2019.114107.
(8) Gartner, E.; Hirao, H. A Review of Alternative Approaches to the Reduction of CO2 Emissions Associated with the Manufacture of the Binder Phase in Concrete. *Cement and Concrete Research* **2015**, *78*, 126–142. https://doi.org/10.1016/j.cemconres.2015.04.012.
(9) Hafez, H.; Kurda, R.; Cheung, W. M.; Nagaratnam, B. A Systematic Review of the Discrepancies in Life Cycle Assessments of Green Concrete. *Applied Sciences* **2019**, *9* (22), 4803. https://doi.org/10.3390/app9224803.
(10) Kendall, A. Time-Adjusted Global Warming Potentials for LCA and Carbon Footprints. *The International Journal of Life Cycle Assessment* **2012**, *17* (8), 1042–1049. https://doi.org/10.1007/s11367-012-0436-5.
(11) Peng, L.; Searchinger, T. D.; Zionts, J.; Waite, R. The Carbon Costs of Global Wood Harvests. *Nature* **2023**, 1–6. https://doi.org/10.1038/s41586-023-06187-1.
(12) Zieger, V.; Lecompte, T.; Hellouin de Menibus, A. Impact of GHGs Temporal Dynamics on the GWP Assessment of Building Materials: A Case Study on Bio-Based and Non-Bio-Based Walls. *Building and Environment* **2020**, *185*, 107210. https://doi.org/10.1016/j.buildenv.2020.107210.
(13) Sproul, E.; Barlow, J.; Quinn, J. C. Time Value of Greenhouse Gas Emissions in Life Cycle Assessment and Techno-Economic Analysis. *Environ. Sci. Technol.* **2019**, *53* (10), 6073–6080. https://doi.org/10.1021/acs.est.9b00514.
(14) O'Hare, M.; Plevin, R. J.; Martin, J. I.; Jones, A. D.; Kendall, A.; Hopson, E. Proper Accounting for Time Increases Crop-Based Biofuels' Greenhouse Gas Deficit versus Petroleum. *Environ. Res. Lett.* **2009**, *4* (2), 024001. https://doi.org/10.1088/1748-9326/4/2/024001.
(15) Lan, K.; Yao, Y. Dynamic Life Cycle Assessment of Energy Technologies under Different Greenhouse Gas Concentration Pathways. *Environ. Sci. Technol.* **2022**, *56* (2), 1395–1404. https://doi.org/10.1021/acs.est.1c05923.
(16) Withey, P.; Johnston, C.; Guo, J. Quantifying the Global Warming Potential of Carbon Dioxide Emissions from Bioenergy with Carbon Capture and Storage. *Renewable and Sustainable Energy Reviews* **2019**, *115*, 109408. https://doi.org/10.1016/j.rser.2019.109408.
(17) Liu, W.; Zhang, Z.; Xie, X.; Yu, Z.; Von Gadow, K.; Xu, J.; Zhao, S.; Yang, Y. Analysis of the Global Warming Potential of Biogenic CO2 Emission in Life Cycle Assessments. *Sci Rep* **2017**, *7* (1), 39857. https://doi.org/10.1038/srep39857.
(18) Albers, A.; Collet, P.; Benoist, A.; Hélias, A. Back to the Future: Dynamic Full Carbon Accounting Applied to Prospective Bioenergy Scenarios. *Int J Life Cycle Assess* **2020**, *25* (7), 1242–1258. https://doi.org/10.1007/s11367-019-01695-7.
(19) Su, S.; Zhu, C.; Li, X.; Wang, Q. Dynamic Global Warming Impact Assessment Integrating Temporal Variables: Application to a Residential Building in China. *Environmental Impact Assessment Review* **2021**, *88*, 106568. https://doi.org/10.1016/j.eiar.2021.106568.
(20) Negishi, K.; Lebert, A.; Almeida, D.; Chevalier, J.; Tiruta-Barna, L. Evaluating Climate Change Pathways through a Building's Lifecycle Based on Dynamic Life Cycle Assessment. *Building and Environment* **2019**, *164*, 106377. https://doi.org/10.1016/j.buildenv.2019.106377.

(21) Collinge, W. O.; Landis, A. E.; Jones, A. K.; Schaefer, L. A.; Bilec, M. M. Dynamic Life Cycle Assessment: Framework and Application to an Institutional Building. *Int J Life Cycle Assess* **2013**, *18* (3), 538–552. https://doi.org/10.1007/s11367-012-0528-2.
(22) Brandão, M.; Kirschbaum, M. U. F.; Cowie, A. L.; Hjuler, S. V. Quantifying the Climate Change Effects of Bioenergy Systems: Comparison of 15 Impact Assessment Methods. *GCB Bioenergy* **2019**, *11* (5), 727–743. https://doi.org/10.1111/gcbb.12593.
(23) CIRAIG. dynCO2: Dynamic Carbon Footprinter, 2010. https://ciraig.org/index.php/project/dynco2-dynamic-carbon-footprinter/ (accessed 2025-02-24).
(24) Van Roijen, E.; Sethares, K.; Kendall, A.; Miller, S. A. The Climate Benefits from Cement Carbonation Are Being Overestimated. *Nat Commun* **2024**, *15* (1), 4848. https://doi.org/10.1038/s41467-024-48965-z.
(25) Lasvaux, S.; Achim, F.; Garat, P.; Peuportier, B.; Chevalier, J.; Habert, G. Correlations in Life Cycle Impact Assessment Methods (LCIA) and Indicators for Construction Materials: What Matters? *Ecological Indicators* **2016**, *67*, 174–182. https://doi.org/10.1016/j.ecolind.2016.01.056.
(26) IPCC. *Climate Change 2014: Synthesis Report. Contribution of Working Groups I, II and III to the Fifth Assessment Report of the Intergovernmental Panel on Climate Change*; Core Writing Team, Pachauri, R. K., Meyer, L. A., Eds.; IPCC: Geneva, Switzerland, 2014.
(27) Kendall, A. Time-Adjusted Global Warming Potentials for LCA and Carbon Footprints. *Int J Life Cycle Assess* **2012**, *17* (8), 1042–1049. https://doi.org/10.1007/s11367-012-0436-5.
(28) Santero, N. J.; Harvey, J.; Horvath, A. Environmental Policy for Long-Life Pavements. *Transportation Research Part D: Transport and Environment* **2011**, *16* (2), 129–136. https://doi.org/10.1016/j.trd.2010.09.005.
(29) Alshqaqeeq, F.; Griffing, E.; Twomey, J.; Overcash, M. Comparing Reusable to Disposable Products: Life Cycle Analysis Metrics. *Journal of Advanced Manufacturing and Processing* **2020**, *2* (4), 1–8. https://doi.org/10.1002/amp2.10065.
(30) Miller, S. A. The Role of Cement Service-Life on the Efficient Use of Resources. *Environmental Research Letters* **2020**, *15* (2). https://doi.org/10.1088/1748-9326/ab639d.
(31) Schuiling, R. D.; Krijgsman, P. Enhanced Weathering: An Effective and Cheap Tool to Sequester CO 2. *Climatic Change* **2006**, *74* (1–3), 349–354. https://doi.org/10.1007/s10584-005-3485-y.
(32) Morales-Vera, R.; Vásquez-Ibarra, L.; Scott, F.; Puettmann, M.; Gustafson, R. Life Cycle Assessment of Bioethanol Production: A Case Study from Poplar Biomass Growth in the U.S. Pacific Northwest. *Fermentation* **2022**, *8* (12), 1–14. https://doi.org/10.3390/fermentation8120734.
(33) Nuss, P.; Eckelman, M. J. Life Cycle Assessment of Metals: A Scientific Synthesis. *PLoS ONE* **2014**, *9* (7), 1–12. https://doi.org/10.1371/journal.pone.0101298.
(34) Van Roijen, E.; Miller, S. A. Towards the Production of Net-Negative Greenhouse Gas Emission Bio-Based Plastics from 2nd and 3rd Generation Feedstocks. *Journal of Cleaner Production* **2024**, *445*, 141203. https://doi.org/10.1016/j.jclepro.2024.141203.
(35) Chen, C. X.; Pierobon, F.; Ganguly, I. Life Cycle Assessment (LCA) of Cross-Laminated Timber (CLT) Produced in Western Washington: The Role of Logistics and Wood Species Mix. *Sustainability (Switzerland)* **2019**, *11* (5). https://doi.org/10.3390/su11051278.
(36) Kane, S.; Miller, S. A. Mass, Enthalpy, and Chemical-Derived Emission Flows in Mineral Processing. *Journal of Industrial Ecology n/a* (n/a). https://doi.org/10.1111/jiec.13476.
(37) Marceau, M. L.; Nisbet, M. A.; Vangeem, M. G. Life Cycle Inventory of Portland Cement Manufacture. *Skokie, IL: Portland Cement Association* **2006**, No. April, 60077–61083.
(38) Guo, R.; Wang, J.; Bing, L.; Tong, D.; Ciais, P.; Davis, S. J.; Andrew, R. M.; Xi, F.; Liu, Z. Global CO 2 Uptake by Cement from 1930 to 2019. **2021**, No. 1, 1791–1805.
(39) Poon, C. S.; Yu, A. T. W.; Jaillon, L. Reducing Building Waste at Construction Sites in Hong Kong. *Construction Management and Economics* **2004**, *22* (5), 461–470. https://doi.org/10.1080/0144619042000202816.

(40) Oner, A.; Akyuz, S. An Experimental Study on Optimum Usage of GGBS for the Compressive Strength of Concrete. *Cement and Concrete Composites* **2007**, *29* (6), 505–514. https://doi.org/10.1016/j.cemconcomp.2007.01.001.
(41) Kim, A.; Cunningham, P. R.; Kamau-Devers, K.; Miller, S. A. OpenConcrete: A Tool for Estimating the Environmental Impacts from Concrete Production. *Environ. Res.: Infrastruct. Sustain.* **2022**, *2* (4), 041001. https://doi.org/10.1088/2634-4505/ac8a6d.
(42) Guggemos, A. A.; Horvath, A. Comparison of Environmental Effects of Steel- and Concrete-Framed Buildings. *J. Infrastruct. Syst.* **2005**, *11* (2), 93–101. https://doi.org/10.1061/(ASCE)1076-0342(2005)11:2(93).
(43) TNO Biobased and Circular Technologies. Phyllis2, Database for (Treated) Biomass, Algae, Feedstocks for Biogas Production and Biochar. https://phyllis.nl/ (accessed 2025-03-07).
(44) Abbas, D.; Handler, R. M. Life-Cycle Assessment of Forest Harvesting and Transportation Operations in Tennessee. *Journal of Cleaner Production* **2018**, *176*, 512–520. https://doi.org/10.1016/j.jclepro.2017.11.238.
(45) Jayalath, A.; Navaratnam, S.; Ngo, T.; Mendis, P.; Hewson, N.; Aye, L. Life Cycle Performance of Cross Laminated Timber Mid-Rise Residential Buildings in Australia. *Energy and Buildings* **2020**, *223*, 110091. https://doi.org/10.1016/j.enbuild.2020.110091.
(46) Yadykova, A. Y.; Ilyin, S. O. Compatibility and Rheology of Bio-Oil Blends with Light and Heavy Crude Oils. *Fuel* **2022**, *314*, 122761. https://doi.org/10.1016/j.fuel.2021.122761.
(47) Carman, J.; Severy, M.; Barrientos, C.; Blasdel, M.; Geronimo, C.; Hsu, C.; Kane, J.; Rios-romero, S.; Wright, M.; Fingerman, K.; Rogers, L.; Comnick, J. *California Biomass Residue Emissions Characterization (C-BREC) Model Framework*; 2021.
(48) Ping, C.-L.; Michaelson, G. J.; Jorgenson, M. T.; Kimble, J. M.; Epstein, H.; Romanovsky, V. E.; Walker, D. A. High Stocks of Soil Organic Carbon in the North American Arctic Region. *Nature Geoscience* **2008**, *1* (9), 615–619. https://doi.org/10.1038/ngeo284.
(49) Chen, C. X.; Pierobon, F.; Ganguly, I. Life Cycle Assessment (LCA) of Cross-Laminated Timber (CLT) Produced in Western Washington: The Role of Logistics and Wood Species Mix. *Sustainability* **2019**, *11* (5), 1278. https://doi.org/10.3390/su11051278.
(50) Lan, K.; Kelley, S. S.; Nepal, P.; Yao, Y. Dynamic Life Cycle Carbon and Energy Analysis for Cross-Laminated Timber in the Southeastern United States. *Environ. Res. Lett.* **2020**, *15* (12), 124036. https://doi.org/10.1088/1748-9326/abc5e6.
(51) O'Dwyer, J.; Walshe, D.; Byrne, K. A. Wood Waste Decomposition in Landfills: An Assessment of Current Knowledge and Implications for Emissions Reporting. *Waste Management* **2018**, *73*, 181–188. https://doi.org/10.1016/j.wasman.2017.12.002.
(52) Shin, B.; Chang, S. J.; Wi, S.; Kim, S. Estimation of Energy Demand and Greenhouse Gas Emission Reduction Effect of Cross-Laminated Timber (CLT) Hybrid Wall Using Life Cycle Assessment for Urban Residential Planning. *Renewable and Sustainable Energy Reviews* **2023**, *185*, 113604. https://doi.org/10.1016/j.rser.2023.113604.
(53) Younis, A.; Dodoo, A. Cross-Laminated Timber for Building Construction: A Life-Cycle-Assessment Overview. *Journal of Building Engineering* **2022**, *52*, 104482. https://doi.org/10.1016/j.jobe.2022.104482.
(54) Cao, Z.; Myers, R. J.; Lupton, R. C.; Duan, H.; Sacchi, R.; Zhou, N.; Reed Miller, T.; Cullen, J. M.; Ge, Q.; Liu, G. The Sponge Effect and Carbon Emission Mitigation Potentials of the Global Cement Cycle. *Nat Commun* **2020**, *11* (1), 3777. https://doi.org/10.1038/s41467-020-17583-w.
(55) GCCA. *Roadmap to Net Zero.*; Global Cement and Concrete Association, 2022. https://gccassociation.org/concretefuture/ (accessed 2023-03-30).
(56) Stripple, H.; Ljungkrantz, C.; Gustafsson, T.; Andersson, R. *CO2 Uptake in Cement-Containing Products*; B 2309; IVL Swedish Environmental Research Institute: Stockholm, Sweden, 2018.

(57) Hawkins, W.; Cooper, S.; Allen, S.; Roynon, J.; Ibell, T. Embodied Carbon Assessment Using a Dynamic Climate Model: Case-Study Comparison of a Concrete, Steel and Timber Building Structure. *Structures* **2021**, *33*, 90–98. https://doi.org/10.1016/j.istruc.2020.12.013.
(58) Ruschi Mendes Saade, M.; Yahia, A.; Amor, B. Is Crushed Concrete Carbonation Significant Enough to Be Considered as a Carbon Mitigation Strategy? *Environ. Res. Lett.* **2022**, *17* (10), 104049. https://doi.org/10.1088/1748-9326/ac9490.
(59) Head, M.; Levasseur, A.; Beauregard, R.; Margni, M. Dynamic Greenhouse Gas Life Cycle Inventory and Impact Profiles of Wood Used in Canadian Buildings. *Building and Environment* **2020**, *173*, 106751. https://doi.org/10.1016/j.buildenv.2020.106751.
(60) Levasseur, A.; Lesage, P.; Margni, M.; Deschênes, L.; Samson, R. Considering Time in LCA: Dynamic LCA and Its Application to Global Warming Impact Assessments. *Environ. Sci. Technol.* **2010**, *44* (8), 3169–3174. https://doi.org/10.1021/es9030003.
(61) Cardellini, G.; Mutel, C. L.; Vial, E.; Muys, B. Temporalis, a Generic Method and Tool for Dynamic Life Cycle Assessment. *Science of The Total Environment* **2018**, *645*, 585–595. https://doi.org/10.1016/j.scitotenv.2018.07.044.
(62) Ericsson, N.; Porsö, C.; Ahlgren, S.; Nordberg, Å.; Sundberg, C.; Hansson, P.-A. Time-Dependent Climate Impact of a Bioenergy System - Methodology Development and Application to Swedish Conditions. *GCB Bioenergy* **2013**, *5* (5), 580–590. https://doi.org/10.1111/gcbb.12031.